Using integrated growth to delineate debris-flow inundation

Mark E. Reid[1*], *Dianne L.* Brien[1], *Collin* Cronkite-Ratcliff[2], and *Jonathan P.* Perkins[2]

[1]U.S. Geological Survey, Volcano Science Center, PO Box 158, Moffett Field, CA, 94035, USA
[2]U.S. Geological Survey, Geology, Minerals, Energy, and Geophysics Science Center, PO Box 158, Moffett Field, CA, 94035, USA

Abstract. Debris-flow volume is fundamental to mobility, yet many debris flows change volume as they travel. Growth can occur through diverse processes such as channel-bed entrainment, bank failures, aggregation of landslides, and coalescence of multiple flows. Integrating growth, either over upslope area or stream length, combines the effects of these growth processes and requires specification of only the growth zone extent and a growth factor. To delineate potential debris-flow inundation, we implement integrated growth factors and simple volume-area relations in a new USGS software package, Grfin Tools. We present two examples of forecasting debris-flow inundation – one using an area growth factor in Puerto Rico and another using a channel-length growth factor in Oregon, USA. The use of growth zones and growth factors enables scenario-based hazard assessments for geomorphic settings with debris-flow growth.

1 Introduction

Debris-flow volume exerts a fundamental control on mobility, speed, momentum, inundation area, and hazard [1-3]. As debris flows travel, they may grow volumetrically and become more destructive in many settings, including steep forested slopes, alpine terrain, post-wildfire burned landscapes, breached glacial lakes, and volcano flanks [4,5]. Growth can vary substantially, sometimes increasing an initial volume by more than an order in magnitude [5,6]. A wide variety of processes can promote growth, including channel-bed erosion and entrainment, incorporation of channel bank failures, aggregation of multiple landslide sources, and hillslope rilling on adjacent slopes [5-8]. Various growth mechanisms may modify a single flow event. Moreover, flow volumes can increase abruptly when multiple flows or surges coalesce from merging channels [8-10].

Explicitly embedding these diverse processes into computational models for debris-flow routing and hazard assessment is an on-going challenge [11-13]. As an alternative, we pursue an empirical modeling approach that allows us to represent the combined effects of various growth processes through growth factors. Here, we use the term *growth factor* to denote spatial growth rates rather than temporal rates. Using pre- and post-debris flow event measurements, integrated growth factors can be measured or estimated over contributing areas or stream-channel lengths where growth occurs [4,14].

Integrated area-growth factors (m^3/m^2), similar to basin erosion or lowering rates, can represent the combined effects of debris-flow growth-inducing processes such as shallow landsliding, rilling, or surface erosion [14,15]. Contributing area can be the entire upslope area or just the region susceptible to providing debris-flow material. Channel-length growth factors (m^3/m), sometimes termed bulking or yield rates, are commonly determined with processes scaled to stream length, such as channel bed entrainment or bank erosion [4,5,16,17]. Growth factors reflect the many conditions promoting debris-flow growth, including steep slopes, the availability of entrainable sediment, and the effects of coalescing flows.

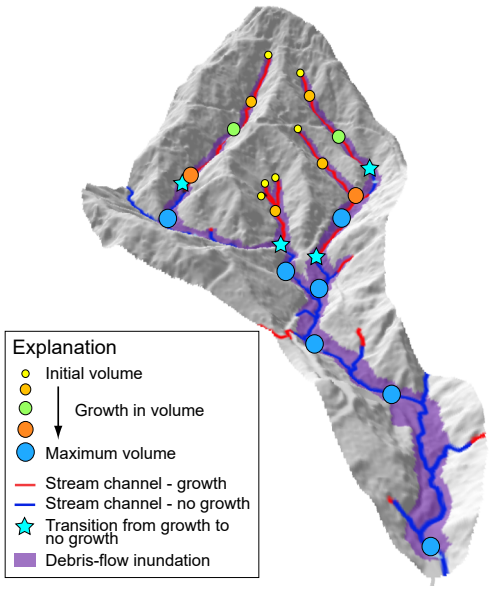

Fig. 1. Perspective view of drainage network showing estimated debris-flow inundation areas and stream-channel zones of volumetric growth and no growth. Dots indicate relative debris-flow volumes. In growth zones, coalescence of flows can abruptly increase flow volume downstream of tributary junctions (e.g. location A). Multiple growth zones can exist in a given channel. In our approach, volume does not change in the no-growth zones. Long axis of area shown is roughly 500 m.

* Corresponding author: mreid@usgs.gov

Zones of debris-flow growth typically occur in the upper part of a basin with steep stream slopes and confined channels [7,18,19] (Fig. 1). As stream slopes decrease farther downstream, growth halts and deposition begins. The transition from growth to deposition commonly ensues in a zone of changing growth, deposition, and sediment transport [16,18,20]. Thus, understanding growth-zone extent and growth-factor magnitude is crucial to forecasting inundation.

2 Inundation using growth factors

To portray the spatial extent of potential debris-flow inundation using integrated growth factors, we use these growth factors within the framework of a simple statistical-empirical method. The inundation mapping approach uses two volume-area power-law equations, one relating debris-flow volume, *V,* to cross-sectional area, *A* (eq. 1), and one to planimetric area, *B* (eq. 2), as used in the Laharz and DFLOWZ models [21-23].

$$A = \alpha_1 V^{2/3} \quad (1)$$
$$B = \alpha_2 V^{2/3} \quad (2)$$

Multiple studies have determined various coefficients, α_1 and α_2, for the volume-area relations (eqs. 1 and 2) using empirical observations from both global and region-specific debris-flow events [24-27]. Some analyses compiled statistics for overall planimetric inundation from the start of a debris flow, thus including potential growth zones [27], even though many of the flows used in these analyses grew as they traveled. Other analyses have emphasized downstream depositional areas after growth had ceased and others have mixed the two approaches [24,25,28].

Several researchers [24,28] have found that volume-area relations derived from these various debris-flow inundation cases have similar power-law coefficients when fit to area with a 2/3 exponent (eqs. 1 and 2). Given these observations, we used the general debris-flow volume-area relations of [27] to determine cross-sectional inundation ($\alpha_1 = 0.1$) in the growth zones and both cross-sectional and planimeteric ($\alpha_2 = 20$) inundation in the no-growth zones.

A fundamental difference in our approach, however, is that we divide the drainage network into regions of volumetric growth and regions of no growth (Fig. 1), rather than specifying a maximum volume. To map inundation, we first define a complete topographic curvature-based drainage network within a digital elevation model. Debris-flow growth zones can then be delineated within the channel network using topographic metrics such as local stream slope and/or stream order (Fig. 1). At each channel network cell within the growth zones, volume (*V*) is computed as the product of either the integrated area-growth factor (c_1) by the upslope area (*U*) or the channel-length growth factor (c_2) by the upstream length (*L*), using either eq. 3 or 4 as described in [4].

$$V = c_1 U \quad (3)$$
$$V = c_2 L \quad (4)$$

At each channel network cell in the growth zones, we use computed volume from the selected growth equations (3 and/or 4) to construct a cross section of inundation roughly perpendicular to the local stream flow direction. To provide smoother plan-view coverage, we also construct two additional cross sections 45º to either side of the perpendicular section. Each section has an area, *A*, based on eq. 1. We then intersect the digital topography with a plan-view circle centered on the channel and having a diameter equal to the average width and a maximum elevation of the three cross sections. The part of this circle with an elevation above the topography is considered inundated. The series of these overlapping circles defines the lateral extent of inundation.

In the no-growth zones, debris-flow volumes at each channel network cell are determined at the downstream end of the adjacent growth zones. We compute cross sections and circles of inundation, as in the growth zones. In addition, we use eq. 2 with the specified volume to define a target total planimetric area, *B*, to be inundated. The total inundation area is delineated by progressing down the channel network, determining cumulative inundation area at each incremental step, and halting when the target area is reached.

We use the USGS software package Grfin Tools (an acronym of growth + flow + inundation), currently under development, to implement this growth/no-growth approach. Grfin Tools is computationally efficient and does not rely on specific GIS software. The above described circle-fitting method minimizes spikey plan-view inundation artifacts in unconfined regions, as can occur with Laharz [4,29].

3 Examples of computed inundation

We present two examples using integrated growth factors for storm-induced debris flows that grew in volume as they traveled through mountainous terrain. Table 1 shows both area and channel-length growth factors for two study areas estimated using detailed mapping of debris flows and DEM differences between repeat aerial photogrammetry or lidar, supplemented by field observations. These growth factors were determined in small areas heavily impacted by debris flows – thus applying these in regional contexts provides relatively "worst cases." Additional measured growth factors for other regions are summarized in [4].

Table 1. Ranges of integrated debris-flow growth factors for two study areas.

	Area-growth factor, c_1 (m^3/m^2)	Channel-length growth factor, c_2 (m^3/m)
Coast Range, Oregon, USA [4]	0.12 to 0.2	11.4 to 24.2
Puerto Rico, USA [14]	0.01 to 0.13	0.7 to 30.4

3.1 Use of area growth

In 2017, Hurricane Maria lashed the island of Puerto Rico in the Caribbean, triggering over 70,000 rainfall-induced landslides; thousands transformed into debris flows and traveled down drainage channels causing widespread damage [30,31]. Debris-flow growth commonly ceased on stream slopes between 3º and 10º [14]. Most flows initiated from shallow landslides and many formed from multiple landslide sources [8,14]. Post-event detailed mapping [32] revealed that landslide transport on hillslopes was commonly extensive, before transitioning into a channelized debris flow (Fig. 2a).

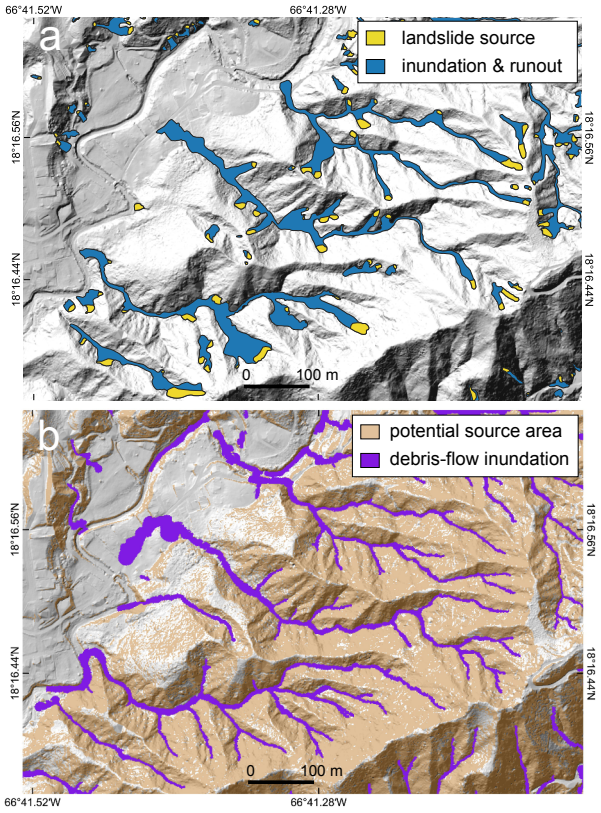

Fig. 2. Example using an area-growth factor in Utuado Municipality, Puerto Rico. (a) Observed landslide sources and debris-flow inundation areas following Hurricane Maria from detailed mapping [32]. (b) Potential shallow-landslide source areas (≥30º slope) and computed debris-flow inundation. Portrayed on hillshade from a 1-m lidar base.

In this example, area-dependent growth processes (e.g., multiple landslides) support the use of an area-growth factor. Fig. 2b portrays debris-flow inundation using a growth factor of 0.01 m^3/m^2 with growth zones defined by channels having stream slopes ≥6º. Area growth is applied to hillslopes ≥30º, similar to observed median slopes for landslide initiation areas [8].

Without calibrating volume-area or growth-factor parameters to match runout observations, our approach is able to delineate reasonable stream-channel inundation areas. The computed runout is slightly larger than observed, due to the use of growth factors from highly impacted areas and relatively extensive growth zones. These conditions tend to over predict basin-wide runout for a specific event due to aggregated effects from growth throughout the entire stream network. However, the delineated areas may be affected in future events.

3.2 Use of channel-length growth

During a large storm in 1996, numerous and widespread debris flows were triggered in the steep and highly dissected terrain of the Oregon Coast Range, USA. Here, debris flows typically originated as shallow landslides in hollows at the heads of drainages before moving down the channel network [33-35]. They grew by entrainment of channel sediment and coalescence of multiple flows [4,9].

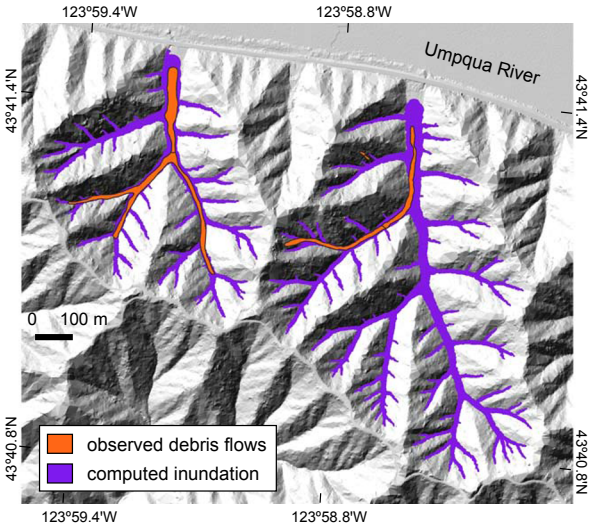

Fig. 3. Example using a channel-length growth factor in the Oregon Coast Range near the Umpqua River. Observed debris-flow inundation from [35]. Computed debris-flow inundation shown for two small basins, as also analyzed in [4]. Portrayed on hillshade from a 0.9-m lidar base.

In this case, channel-dependent growth processes (e.g., bed entrainment) provide an opportunity to examine the use of a channel-length growth factor. We use a channel-length growth factor of 11 m^3/m (Table 1) and growth zones defined by channels with slopes ≥10º (Fig. 3). As in the area-growth example, computed inundation zones are slightly more extensive than observations, due in part to aggregation of growth.

4 Summary

Understanding the magnitude and location of debris-flow growth is crucial to delineating inundation. Many diverse processes can promote growth, and the effects can be integrated over either upslope area or stream length. Using simple growth relations, combined with volume-area relations for defining inundation area (as implemented in Grfin Tools), we illustrate the use of different integrated growth factors in two settings. The combination of relatively simple growth factors and growth zones can generate reasonable inundation zones, suitable for multiple scenario-based hazard assessments in geographic regions having debris-flow growth.

References

1. K. R. Barnhart, R. P. Jones, D. L. George, B. W. McArdell, F. K. Rengers, D. M. Staley, J. W. Kean, J. Geophys. Res., Earth Surf. **126**(12) e2021JF006245 (2021)
2. R. M. Iverson, M. E. Reid, M. Logan, R. G. LaHusen, J. W. Godt, J. P. Griswold, Nature Geosci. **4** 116-121 (2011)
3. J. Corominas, Can. Geotech. J. **33**(2) 260-271 (1996)
4. M. E. Reid, J. A. Coe, D. L. Brien, Geomorphology **273** 396-411 (2016)
5. O. Hungr, S. McDougall, M. Bovis, *Entrainment of material by debris flows*, in *Debris-flow Hazards and Related Phenomena*, edited by M. Jakob, O. Hungr, Springer, Berlin (2005), pp. 135-158
6. P. M. Santi, V. G. deWolfe, J. D. Higgins, S. H. Cannon, J. E. Gartner, Geomorphology **96** 310-321 (2008)
7. J. Theule, F. Liébault, D. Laigle, A. Loye, M. Jaboyedoff, Geomorphology **243** 92-105 (2015)
8. E. K. Bessette-Kirton, J. A. Coe, W. H. Schulz, C. Cerovski-Darriau, M. M. Einbund, Landslides **17**(12) 2795-2809 (2020)
9. J. A. Coe, M. E. Reid, D. L. Brien, J. A. Michael, *Assessment of topographic and drainage network controls on debris-flow travel distance along the west coast of the United States*, in *Proceedings of the 5th International Conference on Debris-Flow Hazards: Mitigation, Mechanics, Prediction and Assessment*, edited by R. Genevois, D.L. Hamilton, A. Prestininzi, Ital. J. Eng. Geol. Env. and Casa Editrice Universita La Sapienza, Rome (2011), pp. 199-209
10. O. Navratil, F. Liébault, H. Bellot, E. Travaglini, J. Theule, G. Chambon, D. Laigle, Geomorphology **201** 157-171 (2013)
11. R. M. Iverson, C. Ouyang, Rev. Geophys. **53**(1) 27-58 (2015)
12. H. Zheng, Z. Shi, S. Yu, X. Fan, K. J. Hanley, S. Feng, Water Resour. Res. **57**(12) e2021WR030707 (2021)
13. Z. Han, B. Su, Y. Li, J. Dou, W. Wang, L. Zhao, Water Res. **182** 116031 (2020)
14. J. A. Coe, E. K. Bessette-Kirton, D. L. Brien, M. E. Reid, *Debris-flow growth in Puerto Rico during Hurricane Maria: Preliminary results from analyses of pre- and post-event lidar data*, in Proceedings of the 13th International Symposium on Landslides, Cartagena, Colombia (2021)
15. A. Dietrich, M. Krautblatter, Earth Surf. Process. Landf. **44**(6) 1346-1361 (2019)
16. C. Scheip, K. Wegmann, Landslides **19**(6) 1297-1319 (2022)
17. L. Marchi, V. D'Agostino, Earth Surf. Process. Landf. **29** 207-220 (2004)
18. R. J. Fannin, M. P. Wise, Can. Geotech. J. **38** 982-994 (2001)
19. L. E. Benda, T. W. Cundy, Can. Geotech. J. **27** 409-417 (1990)
20. K. Morell, P. Alessio, T. Dunne, E. Keller, Geophys. Res. Lett. **48**(24) e2021GL095549 (2021)
21. M. Berti, A. Simoni, Comput. Geosci. **67** 14-23 (2014)
22. S. P. Schilling, *Laharz_py: GIS tools for automated mapping of lahar inundation hazard zones*, USGS Open-File Rep. 2014-1073, (2014)
23. R. M. Iverson, S. P. Schilling, J. W. Vallance, Geol. Soc. Am. Bull. **110** 972-984 (1998)
24. M. Berti, A. Simoni, Geomorphology **90** 144-161 (2007)
25. G. B. Crosta, S. Cucchiaro, P. Frattini, *Validation of semi-empirical relationships for the definition of debris-flow behaviour in granular materials*, in *Proc. 3rd International Conference on Debris-Flow Hazards Mitigation: Mechanics, Prediction, and Assessment*, edited by D. Rickenmann, C.-l. Chen, Millpress, Rotterdam, Netherlands (2003), pp. 821-831
26. D. O. Dorta, G. Toyos, C. Oppenheimer, M. Pareschi, R. Sulpizio, G. Zanchetta, Nat. Hazards **40**(2) 381-396 (2007)
27. J. P. Griswold, R. M. Iverson, *Mobility statistics and automated hazard mapping for debris flows and rock avalanches*, USGS Sci. Investig. Rep. 2007-5276, (2008)
28. A. Simoni, M. Mammoliti, M. Berti, Geomorphology **132**(3-4) 249-259 (2011)
29. E. Muñoz-Salinas, M. Castillo-Rodríguez, V. Manea, M. Manea, D. Palacios, J. Volcanol. Geotherm. Res. **182** 13-22 (2009)
30. K. S. Hughes, W. Schulz, *Map depicting susceptibility to landslides triggered by intense rainfall, Puerto Rico*, USGS Open-File Rep. 2020-1022, (2020)
31. E. K. Bessette-Kirton, C. Cerovski-Darriau, W. H. Schulz, J. A. Coe, J. W. Kean, J. W. Godt, M. A. Thomas, K. S. Hughes, GSA Today **29**(6) 4-10 (2019)
32. M. M. Einbund, K. S. Baxstrom, W. H. Schulz, *Map data from landslides triggered by Hurricane Maria in four study areas in the Lares Municipality, Puerto Rico*, USGS data release, (2021)
33. C. L. May, R. E. Gresswell, Geomorphology **57** 135-149 (2004)
34. D. R. Montgomery, K. M. Schmidt, W. E. Dietrich, J. McKean, J. Geophys. Res. **114**(F01031) (2009)
35. J. A. Coe, J. A. Michael, M. M. Burgos, *Map of debris flows caused by rainfall during 1996 in parts of the Reedsport and Dear Head Point quadrangles, Douglas County, southern Coast Range, Oregon*, USGS Open-File Rep. 2011-1150, (2011)